NUMERICAL AND EXPERIMENTAL EVALUATION OF VENTILATION IN LABORATORIES: A CASE STUDY

Glenn Reynders, Dirk Saelens
Building Physics Section, Department of Civil Engineering, K.U.Leuven, Belgium.

Abstract

Ventilation is a key performance requirement in laboratory design as it has to guarantee a safe and comfortable indoor environment. Current standards and guidelines on laboratory ventilation often impose high ventilation rates, increasing the energy need for ventilation, the environmental impact and the energy costs, at many large research facilities. This research focuses on the intra-zonal airflow in a standard laboratory set-up. The airflow and ventilation efficiency is computed with Computational Fluid Dynamics (CFD) and an extensive in-situ experimental case, in which different ventilation strategies are evaluated, has been conducted. The results indicate that the current design standards, which impose a minimal number of air changes per hour, cannot guarantee an optimal, energy efficient design. An optimal design starts from a comprehensive risk analysis. The CFD-simulations and experimental study show that an optimal design should not only be based on a minimal ventilation rate but also has to include an analysis of the impact of the location and type of the ventilation inlet and outlet, the room geometry and ideally the influence of occupants and laboratory appliances. Therefore, it can be concluded that a reformulation of the requirements for laboratory ventilation is appropriate, which in practice will lead to an increasing complexity of the ventilation design process. Although they require a good comprehension and implementation of correct physical properties, CFD-simulations are expected to become an interesting and even mandatory design tool for future, energy efficient laboratory ventilation.

Keywords: ventilation, indoor air quality, cfd, tracer-gas, mean age of air

1 Introduction

The last decade, interest in energy efficient building design has increased rapidly due to climate change issues. The high energy use in research laboratories gives rise to a large potential for energy saving strategies for these facilities. In the search for energy efficient laboratories, ventilation plays a main role as it is one of the largest factors in the total energy use of laboratory facilities. For instance, at the University of Leuven, which houses numerous laboratories in its infrastructure, ventilation of laboratories is responsible for 25 % of the total primary energy use of the university, or 79 000 GJ per year. Optimization of the ventilation design in laboratories therefore shows a large potential for energy savings.

Where most research has focused on the design, standardization and implementation of high performance, VAV fume hoods (Mills et al., 2005, Bell, 2008), major energy savings can be achieved by optimizing the general-purpose ventilation strategies. In a case study Memarzadeh (2009) estimates the energy savings resulting from a decrease of the ventilation rate. Reducing the air change rate, from 12 ACH to 6 ACH, results in an energy saving of 49 %. In addition to a lower air change rate literature often suggests an implementation of demand controlled ventilation strategies (Sharp, 2010). Since hazardous situations only occur during a small percentage of the working hours, Sharp found that an increase of the air change rate is only needed about 1 % of the time.

However, lowering the ventilation rate cannot be done without considering safety and indoor air quality (Hall et al., 1998, Bretherick et al., 2007).

Although there is no fundamental discussion on the importance of ventilation for laboratory safety, design guides and building codes are often vague on the minimal ventilation requirements that lead to a safe indoor environment. They often use a conservative approach and rules of thumb based on simplified global air-mixing models. For example, ASHRAE applications suggests a ventilation rate varying between 6 ACH and 12 ACH (ASHRAE, 2007). NFPA-24-2004 demands 8 ACH in occupied conditions and 4 ACH when the laboratory is unoccupied (NFPA, 2004). The European standard EN 13779 does not propose a minimal number of ACH, but claims that the ventilation rate is best calculated based on data of the contaminant emission rates (CEN, 2004). ANSI/AIHA Z9.5 states contaminant control is not primarily done by ventilation, but by specific measurements at the source. Therefore the ventilation rate should be established or agreed upon by the owner (ANSI/AHIA Z9.5, 2002).

Where most standards and codes impose a minimal number of air changes per hour, recent laboratory design guides reject this approach: “ASHRAE: laboratory design guide” (McIntosh et al., 2001) suggests a ventilation design based on a risk analysis. A comprehensive study, identifying potential hazards and various control measures, has to result in minimal design requirements for the ventilation system. This paper evaluates the relevance of air change rates based on standards to assess effectiveness of ventilation. By numerical simulations of the intra-zonal airflow, using computational fluid dynamics (CFD) and a comprehensive experimental case study, we identify some fundamental problems encountered with these simplified standards.

2 Methodology

Both numerical simulations and an experimental study are carried out on a laboratory set-up that is commonly found at the research department of the university hospital of the K.U.Leuven. The laboratory used for the experimental study measures 8.40x3.40x3.40 m³, has one exterior wall facing north-west and was empty due to renovations. To establish a room volume that was closer to the model used in the numerical simulations, part of the laboratory, near the outer wall, was air-tight sealed, reducing the length to 7 m. Laboratory tables are placed at both sides of the room as shown in figure 2.

The numerical simulations are carried out on a simplified model of the laboratory, shown in figure 1. The dimensions of the room differ from the experimental geometry since the numerical simulations were carried out before the exact location for the experiments was known. The laboratory model has a length of 6 m, a width of 3 m and a height of 3.5 m. As for the experimental study, two workbenches are placed at both sides of the room and modeled as airtight volumes. Each workbench has a height of 1.10 m and a width of 0.90 m. The ventilation inlet and outlet consist of two grilles placed at the opposite walls on the symmetry plane.

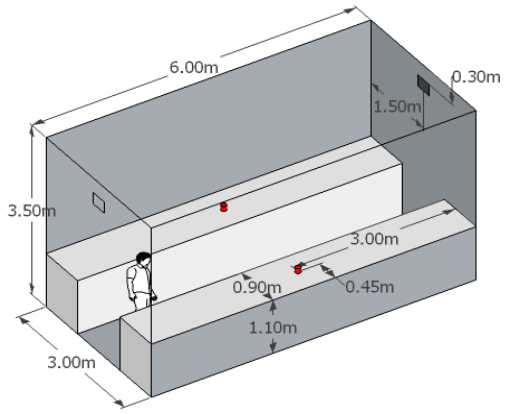

Figure 1. Simplified laboratory geometry used for the numerical simulations

Figure 2. Laboratory set-up for the experimental study

2.1 Numerical simulations

The numerical simulations focus on the removal of a contaminant by the ventilation system. The importance of minimal air change rates for the effectiveness of contaminant removal is evaluated in different test-cases. The air change rates used in these test-cases are 4 ACH, 8 ACH and 16 ACH. With a total volume of 63 m³ this results in an airflow rate of 252 m³/h, 504 m³/h and 1008 m³/h respectively. For each air change rate, the dimensions of the grill have been determined to guarantee a proper air velocity at the inlet, taking into account the throw of the supply. The properties are summarized in table 1. Notice the differences between the effective and nominal area of the grilles. The nominal areas are based on the outer dimensions of the grille, whereas the effective area only takes into account the effective openings, as specified by the product information.

The spill is located at the centre of the workbench, as shown in figure 1 and represents a container with a diameter of 0.05 m that remains open. The contaminant production rate was calculated as an evaporation problem using Stefan's law:

$$\ln \frac{p_t}{p_t - p_{S0}} = N_s \frac{RT}{D_s p_t} H \tag{1}$$

where p_t [Pa] is the atmospheric pressure, p_{S0} [Pa] is the saturated vapor pressure of contaminant S, N_S [mol/m²s]is the production rate , D_s is the diffusion coefficient and H [m] is the height of the container (Rietma, 1976). For ethanol a production rate of $6.62e^{-4}$ kg/h is found. This production rate is introduced to the numerical model by introducing a source term at the cells which represent the container. The production rate was the same for all simulated contaminants.

Intra-zonal airflow simulations are carried out using ANSYS FLUENT 12.1. The governing equations in these simulations are the continuity equation for mass transfer, the transient RANS-equations for momentum transfer, the thermal energy equation for heat transfer and the equation for species transfer. For transient flow of incompressible fluids, these equations can be generalized as:

$$\frac{\partial}{\partial t}\rho\phi + \frac{\partial}{\partial \mathrm{x_i}}\rho U_i \phi = \frac{\partial}{\partial \mathrm{x_i}}\left(\Gamma_\phi \frac{\partial \phi}{\partial x_i}\right) + S_\phi \tag{2}$$

where Γ_ϕ is the diffusion coefficient and S_ϕ represents source terms of the dependent variable ϕ (Fluent, 2009). To solve the closure problem, two additional equations are coupled to the given set of governing equations by the turbulence model. Several turbulence models where compared in this study: standard k-ϵ model, RNG-k-ϵ model, Realizable k-ϵ model, standard k-ω model and SST k-ω model (Zhai, 2007). A sensitivity analysis (Reynders, 2010) showed good resemblance between the different models, however due to the difference between the experimental and the numerical set-up, no validation data were available. The results, discussed below, are obtained with the RNG k-ϵ model, as it is found to perform well for indoor airflow simulations (Zhai, 2007) and needed less computational effort than e.g. the SST k-ω model.

Boundary conditions for the airflow are specified at the ventilation inlet and outlet and no-slip boundary conditions are used on the walls and workbench surfaces. The air supply is modeled as a velocity inlet. The supply velocity is given by:

$$v_{inlet} = \frac{Q}{A_0}\ [m/s] \tag{3}$$

where Q is the flow rate [m³/s] and A_0 [m²] represents the nominal area of the grille. The turbulence intensity (T_i) is estimated by:

$$T_i = 0.16\, Re_{D_H}^{-\frac{1}{8}} \tag{4}$$

where Re_{D_H} is the Reynolds number based on the hydraulic diameter of the supply opening, resulting in a T_i of 4.4 % for 8 ACH. The turbulent length scale is coupled to the ventilation grille's geometrical properties, which results in a turbulent length scale l of 0.02 m. A sensitivity study on the inlet boundary conditions has been carried out showing an important influence on the flow pattern and

Table 1. Properties grilles in simulations

Air flow [m³/h]	Effective Area [m²]	Nominal Area [m²]
252	0.021	0.041
504	0.043	0.073
1008	0.125	0.203

Table 2. Overview of experimental test-cases

ACH / Type of supply	4 ACH	8 ACH	16 ACH
Grille diffuser	1A	1B	1C
Swirl diffusers	2A	2B	2C
Air-sock	3A	3B	3C

velocities (Reynders, 2010). The supply air temperature is derived from the cooling load. Internal gains are estimated at 25 W/m² and are distributed over the floor and the work surfaces, resulting in a total cooling load of 450 W. The influence of bouyancy effects is found important, due to the low velocities near the floor and work surfaces. To obtain a Richardson-number lower than 0.1, for which thermal effects do not influence the flow pattern, only a temperature difference of 0.2 °C between the surface and the air, was allowed. Therefore buoyancy effects are taken into account by taking to account the energy equation and modeling the density of the fluid using the "incompressible-ideal-gas" model (Fluent, 2009).

The computational grid is constructed using the "MultiZone"-method from the "ANSYS Workbench Mesher." This resulted in a hexagonal grid with 98 700 elements, a maximal skewness of 2.30×10^{-3} and a maximal aspect ratio of 2.02. Different meshes were tested in a grid convergence problem. The discretization error, estimated using the Richardson extrapolation method, is found to be less than 5% (Reynders, 2010).

In order to limit the computational time, the airflow close to the wall is calculated by using standard wall functions instead of enhanced wall treatment. It has to be pointed out that the requirements for y+ are not achieved for the whole domain. The applications of standard wall functions demands for the first node to be situated in the turbulent zone, i.e. y+ > 30. Due to the velocity drops near the room's corners, y+ in these areas is found to be smaller, resulting in an overestimation of the air velocity near the wall. However, for the scope of this research, these effects are found to play no major role.

2.2 Experimental study

Where the numerical simulations focuses on the influence of the air change rate on the contaminant removal due to a spill, the experimental study completes these results with an analysis of the distribution of fresh air for different ventilation techniques. Three different supply systems are tested for three different flow rates, resulting in 9 different test cases, summarized in table 2.

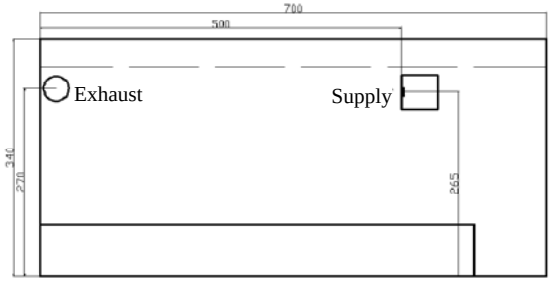

Figure 3. Laboratory geometry and setup with grille diffuser

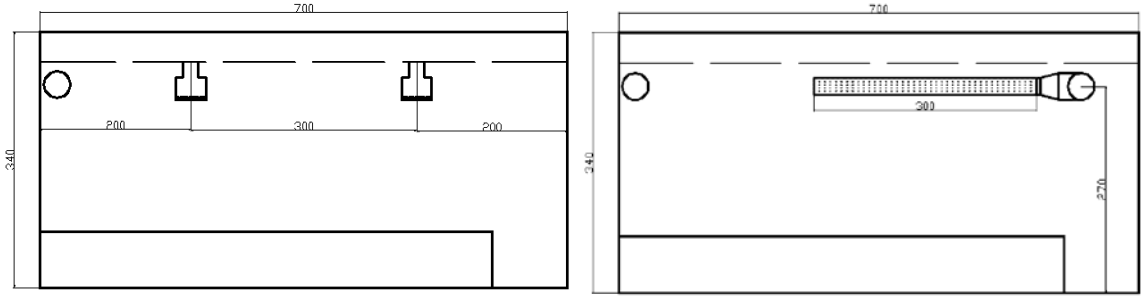

Figure 4. Laboratory geometry and setup with swirl diffusers (left) and air-sock (right)

The first technique consists of a grill diffuser. A similar technique is used in the numerical study. This diffuser is placed in the symmetry plane at one side of the room, as shown in figure 3. The exhaust grilles, indicated on this figure, are the original laboratory exhaust grilles. These two grilles are placed immediately on the exhaust duct and will be used for all tested cases. The exhaust flow rate can be controlled by adjusting the grill openings. The supply flow rate can be adjusted using a valve in the supply duct.

The second supply system uses two swirl diffusers. These diffusers are placed symmetrically in the room to provide an optimal distribution of fresh air, as shown in figure 4 (left). To achieve an appropriate velocity distribution, or throw, the correct diffuser type has to be selected in accordance to the flow rate. This was done not only for the swirl diffusers but also for the grille diffusers.

The third supply system is the air-sock, shown in figure 4 (right). Air-socks are perforated textile ducts used for draught-free air distribution. The large percentage of perforations makes it possible to supply large flow rates at low air velocities, making it an interesting technique for laboratories. The air-sock used in this study had a length of 3 m and was designed for a flow rate of 1000 m³/h, which was the maximal flow rate aimed at in this experimental study.

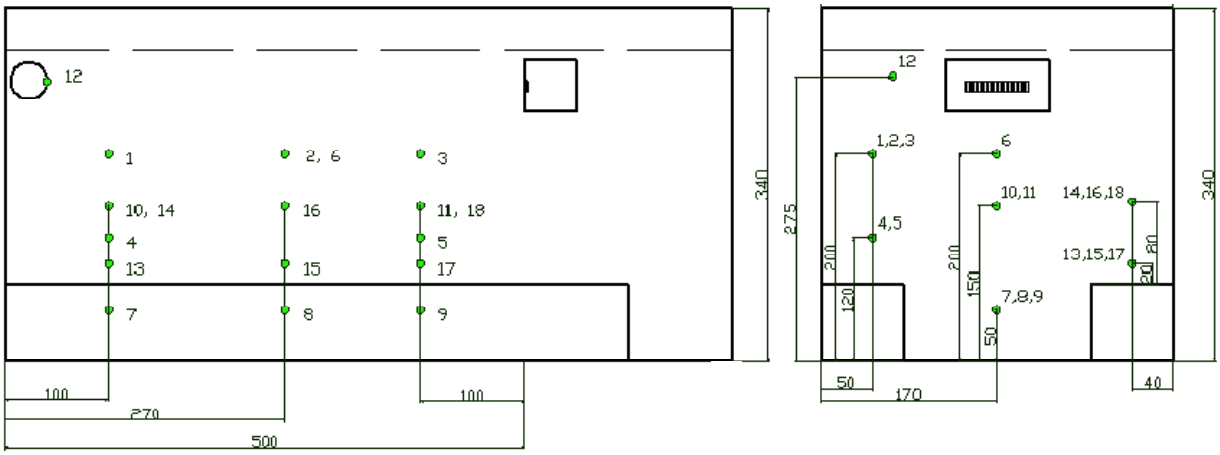

Figure 5. Locations of sample points for tracer-gas measurements

The focus of the experimental study lies within the analysis of the fresh air distribution. For this a tracer (SF_6) is injected at the supply duct, with a constant emission rate. The fresh supply air is thereby marked with SF_6, which allows monitoring the distribution of fresh air into the laboratory. For the tracer measurements the Bruël & Kjaer Innova type 1303 was used for sampling and dosing the SF_6-tracer. This allowed a set of 6 points to be measured in one phase. In total every case is measured 3 times, resulting in 18 different sample points, shown in figure 5. The concentration in each point is monitored by the Bruël & Kjaer multi-gas monitor type 1302. This monitor uses photo-acoustic infra-red detection to measure the SF_6-concentration, with an accuracy of 10^{-2} ppm. By stopping the tracer supply after achieving constant concentrations and monitoring the concentration decay ($c_p(t)$) the local mean age of air (τ_p), can be derived as:

$$\tau_p = \frac{\int_0^\infty c_p(t)dt}{c_p(0)} \tag{5}$$

The local mean age of air expresses how long an air molecule has travelled to reach the sample point, starting from the air supply. The efficiency of the ventilation (ϵ) is calculated by the ratio of the local mean age of air to the mean age of air. The latter is defined as:

$$\tau = \frac{1}{Q_{exhaust}} \tag{6}$$

In addition to the tracer-gas concentration also relative humidity, temperature and air velocity where measured. The air velocity was measured in three reference points using hot-sphere anemometers.

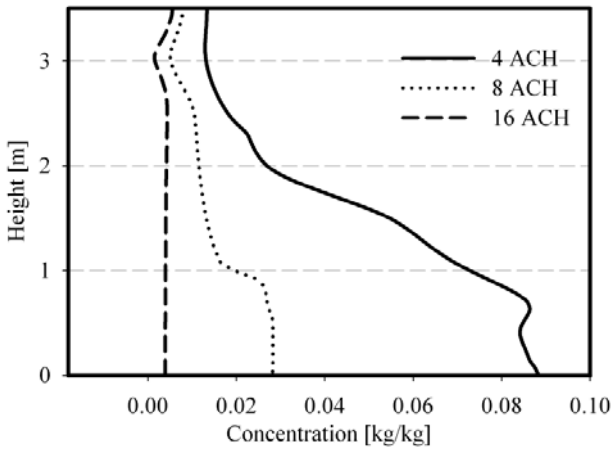

Figure 6. Concentrations of dicloromethane for different air change rates at the center of the room

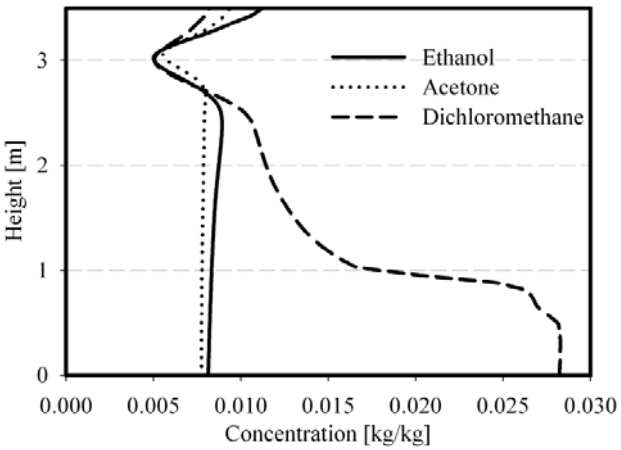

Figure 7. Concentrations of ethanol, aceton and dichloromethane at 8 ACH at the center of the room

3 Results

3.1 Numerical simulations

The case-study shown in this paper investigates the contaminant dispersion due to a point source located in the middle of the workbench. Figure 8 shows the airflow in the symmetry plane of the room obtained by the transient numerical model from §2.2. Two zones can be distinguished in the air flow pattern. The first zone is located near the ceiling and is characterized by the supply jet stream. A relative large fraction of the fresh air is immediately extracted by the exhaust, resulting in relative low air velocities in the room. This indicates that the assumption of perfect mixture, which is used for most of the simplified design standards, overestimates the ventilation efficiency.

Also the density of the contaminant influences the effectiveness of removal. Therefore the simulations used three different contaminants, selected by their molecular weight: ethanol (46.02 g/mol), acetone (58.08 g/mol) and dichloromethane (84.93 g/mol). At an air change rate of 8 ACH, figure 7 shows that the ventilation strategy, with an exhaust near the ceiling, cannot efficiently remove contaminants with a density larger than the density of air. This problem is even more important as the ventilation rate is lowered to 4 ACH, as shown in figure 6. Although ethanol is expected to be removed more easily, figure 7 shows slightly better results for acetone. This can be explained by the small differences in the airflow pattern which shows higher local velocities for the acetone case. A larger velocity near the contaminant source therefore improves the removal of the contaminant. This again emphasizes the importance of a well designed intra-zonal air distribution.

Increasing the air change rate to 16 ACH prevents the heavy dichloromethane from descending towards the floor, although the threshold level of 0.21 g/kg is not reached. This can be explained by the large amount of fresh air which is extracted before mixing with the contaminated room air, resulting in low ventilation efficiencies.

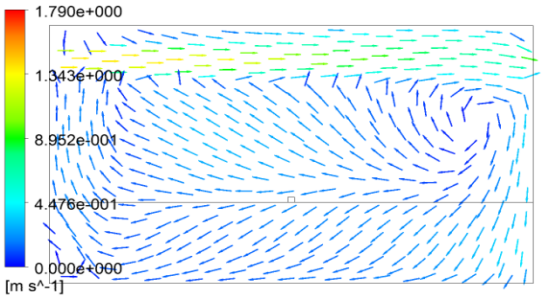

Figure 8. Velocity field for 16 ACH at the symmetry plane

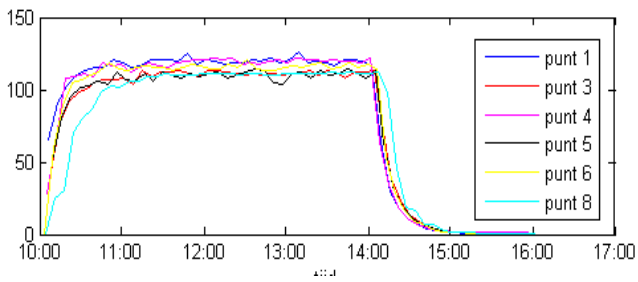

Figure 9. Tracer-gas results for test-case 1C

3.4 Experimental Case study

Similar as for the numerical simulations, the tracer-gas experiments show that a better indoor air quality, i.e. lower concentrations on breathing height, can be achieved by increasing the air change rate in a laboratory. The results, presented in table 3, show how the local mean age of air decreases when the air flow is increased from 265 to 565 m³/h. There is however no linear relationship between the local mean age of air and the air change rate, shown by the efficiency. The short circuiting of supply air directly to the exhaust, which was also found important in the numerical simulations, results in an efficiency of ventilation that is up to 54 % below what would be expected in a perfect mixing situation. For test-case 2C, due to this low efficiency, no real improvements can be found in the local mean age of air than compared with test-case 2B. An optimal design of the ventilation system, more carefully concerning the intra-zonal air distribution, could make it possible to improve this efficiency drastically.

The measurements for the swirl diffusers and the air-sock show interesting results near the floor, i.e. point 7, 8 and 9. Both types of supply have problems to provide fresh air near the floor area. Although the results of 3B show acceptable results for point 7 and 9, the local mean age of air is about 60 % higher for point 8. This can be explained by analyzing the temperature distribution in the room. These show that for point 8, which was measured during the afternoon, the unconditioned, supply temperature is higher than the room temperature. Therefore the fresh air will remain in the upper regions of the laboratory due to buoyancy effects. For point 7 and 9, which were measured over night the supply temperature was lower than the room temperature allowing the fresh air to descend to the floor. Although the distribution of fresh air is of more importance at breathing level than near the floor, the numerical simulations have shown the importance of air velocity to extract contaminants out of the room. The results for the swirl diffusers and the air-sock indicate potential problems for a spill near the floor. For the points above the workbenches, the swirl diffusers showed the best results.

4 Conclusion

Numerical simulations on a simplified laboratory geometry showed how the basic assumption of perfect mixing conditions, overestimate the performance of the laboratory ventilation. One of the major factors influencing the efficiency is the amount of fresh air that is immediately extracted, without mixing with the room air. The simulations also showed the importance of the exhaust location. The relative small air velocity air is not able to transport the contaminants to exhaust located

Table 3. Summary of tracer-gas measurements test-cases 1B, 2A, 2B, 2C and 3B

	1B: 592 *m³/h*		2A: 264 *m³/h*		2B: 565 *m³/h*		2C: 1010 *m³/h*		3B: 600 *m³/h*	
point	τ_p [h]	Efficiency [%]	τ_p [h]	Efficiency [%]	τ_p [h]	Efficiency [%]	τ_p [h]	Efficiency [%]	τ_p [h]	Efficiency [%]
1	0.17	74	0.27	104	0.29	46	0.25	30	0.21	58
2	0.19	67			0.15	88	0.20	37	0.20	62
3	0.17	73	0.21	137	0.15	87	0.13	58	0.20	63
4	0.22	56	0.24	120	0.25	53	0.36	20	0.23	53
5	0.15	82	0.34	85	0.16	83	0.31	23	0.18	69
6	0.14	87	0.38	74	0.14	94	0.14	51	0.18	68
7	0.16	78	0.39	74	0.26	50	0.19	39	0.19	66
8	0.16	77	0.41	70	0.15	90	0.28	26	0.26	48
9	0.18	70	0.33	85	0.22	60	0.13	58	0.13	97
10	0.18	69	0.34	85	0.18	73	0.18	42	0.18	70
11	0.15	86	0.39	73	0.17	76	0.14	52	0.14	88
12	0.14	92			0.11	118	0.14	54	0.14	91
13			0.36	80	0.17	75	0.16	45	0.23	53
14			0.28	100	0.14	91	0.15	47	0.16	77
15			0.25	113	0.12	112	0.13	57	0.20	62
16			0.29	97	0.19	69	0.12	60	0.28	44
17			0.29	99	0.16	82	0.12	60	0.19	63
18			0.47	61	0.15	85	0.14	54	0.23	53

in the upper region of the room. This effect becomes even more important as the density of the contaminant increases.

The experimental study confirms these results as it shows that the efficiency of the different supply systems is strongly influenced by the amount of air that is directly extracted to the exhaust. Close to the floor the swirl diffusers and air-sock showed very low efficiencies. The amount of fresh are that was able to penetrate into the floor region was influenced by the temperature. Showing the worst results when the inlet temperature was higher than the air temperature in the room.

The numerical and experimental study both show that standards based on rules of thumb for the air change rate cannot guarantee an optimal ventilation strategy. Even more, since they don't take in to account the efficiency and intra-zonal air distribution, those standards cannot guarantee the laboratory air quality and therefore the laboratory safety. A conservative air change rate is therefore required resulting in an increase of the energy use.

To allow an optimal ventilation design, more specific performance requirements need to be specified. These requirements must be deduced from an extensive risk analysis for the laboratory, taking into account the different materials and procedures that can cause hazardous situations. A case specific ventilation design has to be made, e.g. taking into account the laboratory topology, location of inlet and outlet, type of supply, thermal requirements, influence of laboratory equipment, influence of personnel, etc. As shown in this research, CFD can become an important design tool in this process. Since this a design process is performance based, it will make place for different optimization techniques, resulting in an optimal solution for laboratory ventilation that is both safe and energy efficient.

5 References

ANSI/AIHA Z9.5 (2002) *American National Standard for Laboratory Ventilation*.

ASHRAE (2009) *ASHRAE Handbook: Fundamentals*. ASHRAE, Inc, Atlanta.

ASHRAE (2007) *ASHRAE Handbook: HVAC applications.* ASHRAE, Inc., Atlanta.

Bell GC. (2008) *Laboratories for the 21st century: best practice guide,* Retrieved from: 'http://www.labs21century.gov/pdf/bp_opt_vent_508.pdf', last accessed: 17/01/11.

Bretherick L., Urben P.G., Pitt M.J. (2007) *Bretherick handbook of reactive chemical hazards*. 7th edition, Elsevier, Oxford.

CEN. (2004) *EN 13779: Ventilation for non-residential buildings – performance requirements for ventilation and room-conditioning systems*. European committee for standardisation (CEN).

Fluent. (2009) *Ansys Fluent 12.0. Documentation.* Fluent, Inc.

Hall J., Gilligan A., Schimmel T., Cecchi M. Cohen J. (1998) *The origin, effects and control of air pollution in laboratories used for human embryo culture,* Human Reproduction 13: 145-155

McIntosh I.D.B., Dorgan C.B., Dorgan C.E. (2001) *ASHRAE Laboratory design guide*. ASHRAE, Inc. Atlanta.

Memarzadeh, F. (2009) *Effect of reducing ventilation rate on indoor air quality and energy cost in laboratories*, Journal of Chemical Health & Safety 16: 20-26

Mills E., Sartor D.A. (2005) *Energy use and savings potential for laboratory fume hoods*, Energy 30: 1859-1864.

NFPA. (2004) *NFPA-45-2004: Standard on fire protection for laboratories using chemicals*. National Fire Protection Association.

Reynders, G. (2010) *Evaluation of ventilation in laboratories*. Master thesis, K.U.Leuven.

Rietma, K. (1976) *Fysische transport- en overdrachtsverschijnselen*. Het Spectrum, Antwerp

Sharp, G.P. (2010) *Demand-based control of lab air change rates,* ASHRAE Journal 52(2): 30-41

Zhai Z., Zhang Z., Zhang W., Chen Q. (2007) *Evaluation of Various Turbulence Models in Predicting Airflow and Turbulence in Enclosed Environments by CFD: Part-1,* HVAC&R Research, 13(6): 853-870